

Exact quantum dynamics study of the $H(^2S)+SiH^+(X^1\Sigma^+)$ reaction on a new potential energy surface of $SiH_2^+(X^2A_1)$

Wen-Li Zhao(赵文丽), Rui-Shan Tan(谭瑞山), Xue-Cheng Cao(曹学成), Feng Gao(高峰), and Qing-Tian Meng(孟庆田)

Citation: Chin. Phys. B, 2021, 30 (**12**): 123403. DOI: 10.1088/1674-1056/ac1b8c
Journal homepage: http://cpb.iphy.ac.cn; http://iopscience.iop.org/cpb

What follows is a list of articles you may be interested in

Quasi-classical trajectory study of H+LiH (v=0, 1, 2, j=0)→Li+H_2 reaction on a new global potential energy surface

Yu-Liang Wang(王玉良), De-Zhi Su(宿德志), Cun-Hai Liu(刘存海), Hui Li(李慧)
Chin. Phys. B, 2019, 28 (**8**): 083402. DOI: 10.1088/1674-1056/28/8/083402

Non-adiabatic quantum dynamical studies of Na(3p)+HD(v=1, j=0)→NaH/NaD+D/H reaction

Yue-Pei Wen(温月佩), Bayaer Buren(布仁巴雅尔), Mao-Du Chen(陈茂笃)
Chin. Phys. B, 2019, 28 (**6**): 063401. DOI: 10.1088/1674-1056/28/6/063401

Isotope effect and Coriolis coupling effect forthe Li + H(D)Cl→LiCl + H(D) reaction

Hongsheng Zhai(翟红生), Guanglei Liang(梁广雷), Junxia Ding(丁俊霞), Yufang Liu(刘玉芳)
Chin. Phys. B, 2019, 28 (**5**): 053401. DOI: 10.1088/1674-1056/28/5/053401

Influence of electron correlations on double-capture process in proton helium collisions

Hoda Ghavaminia, Ebrahim Ghanbari-Adivi
Chin. Phys. B, 2015, 24 (**7**): 073401. DOI: 10.1088/1674-1056/24/7/073401

Quasi-classical trajectory investigation on the stereodynamics of Li+DF (v=1-6, j=0)→LiF+D reaction

Zhang Ying-Ying, Li Shu-Juan, Shi Ying, Xie Ting-Xian, Jin Ming-Xing
Chin. Phys. B, 2014, 23 (**12**): 123402. DOI: 10.1088/1674-1056/23/12/123402

Exact quantum dynamics study of the $H(^2S) + SiH^+(X^1\Sigma^+)$ reaction on a new potential energy surface of $SiH_2^+(X^2A_1)$*

Wen-Li Zhao(赵文丽)[1], Rui-Shan Tan(谭瑞山)[2], Xue-Cheng Cao(曹学成)[1], Feng Gao(高峰)[1,†], and Qing-Tian Meng(孟庆田)[3,‡]

[1] School of Information Science and Engineering, Shandong Agricultural University, Taian 271018, China
[2] Department of Science, Shandong Jianzhu University, Jinan 250101, China
[3] School of Physics and Electronics, Shandong Normal University, Jinan 250358, China

(Received 17 June 2021; revised manuscript received 26 July 2021; accepted manuscript online 7 August 2021)

Based on a new global potential energy surface of $SiH_2^+(X^2A_1)$, the exact quantum dynamical calculation for the $H(^2S) + SiH^+(X^1\Sigma^+) \rightarrow H_2 + Si^+$ reaction has been carried out by using the Chebyshev wave packet method. The initial state specified ($v_i = 0$, $j_i = 0$) probabilities, integral cross sections (ICS) and thermal rate constants of the title reaction are calculated. All partial wave contributions up to $J = 90$ are calculated in exact quantum calculation including the full Coriolis coupling (CC) effect. The dynamical behaviors of probabilities, ICSs and rate constants are found to be in accord with an exothermic reaction without potential barrier. By comparing the probabilities of CC with the corresponding centrifugal sudden (CS) approximation ones, it can be concluded that neglecting CC effect will decrease the collision time, increase the amplitude of oscillation and lead to overestimation or underestimation of the reaction probability. For ICSs and rate constants, it is found that the deviation of CC and CS ICSs is small in the most of collision energy range except for the range of 0 eV–0.05 eV, while the deviation of both rate constants is considerable in the temperature range of 16 K–1000 K.

Keywords: Chebyshev wave packet method, reaction probability, integral cross section, rate constant

PACS: 34.50.Lf, 82.20.Db, 82.20.Pm **DOI:** 10.1088/1674-1056/ac1b8c

1. Introduction

During the past decades, the construction of accurate global potential energy surface (PES) of the methylene ion CH_2^+ and related dynamics investigation have aroused great interest because of their importance in atmospheric chemistry and astrophysics.[1–6] Comparatively speaking, the global PES of SiH_2^+ system and related dynamical calculations are seldom reported. For the silicon semiconductor industry, SiH^+ and H are known to be two reactive intermediate species in chemical-vapor deposition process, and the investigation on $H + SiH^+$ reaction is of great practical significance.[7] Furthermore, SiH^+ and H are known to be abundant in interstellar space, and the study of $H + SiH^+$ reaction can help us understand the physical and chemical processes taking place in astrophysics.[8] In 2019, our research team[9] firstly reported an accurate global ground state PES (hereafter GMS-PES) for $SiH_2^+(X^2A_1)$ at multireference configuration interaction level including Davidson corrections by the many-body expansion method. Using the coupled states (CS) approximation, we also carried out Chebyshev wave packet dynamical calculations for the reaction

$$H(^2S) + SiH^+(X^1\Sigma^+) \rightarrow Si^+(^2P) + H_2(X^1\Sigma_g^+). \quad (1)$$

However, the CS approximation has been proved to be inaccurate in some chemical reactions due to neglecting the Coriolis coupling (CC) effect.[10,11] In order to obtain accurate dynamical results and quantitatively investigate the influence of CC effect on the $H + SiH^+$ reaction, an accurate Chebyshev wave packet calculation considering full CC effect is performed based on GMS-PES of $SiH_2^+(X^2A_1)$ in this work.

It should be noted that there are no experimental and other theoretical results of $H + SiH^+$ reaction up to date. Therefore, we briefly review some experimental and theoretical results of other reactions associated with the title reaction as follows. From the experimental side, Elkind and Armentrout[12] measured the total cross section as a function of reactant kinetic energy of $Si^+(^2P) + H_2\left(X^1\Sigma_g^+\right) \rightarrow SiH^+ + H$ reaction with a guided ion beam mass spectrometer and obtained the bond energy for SiH^+ subsequently. In 1985, Si^+ and SiH^+ were monitored in a laser photo fragmentation spectroscopic investigation of SiH_2^+ ion by Curtis *et al.*,[13] which indicated that SiH_2^+ ion can dissociate into two competitively chemical channels, $H + SiH^+$ and $Si^+ + H_2$.

From the theoretical point of view, with multi-reference configuration interaction (MRCI) calculation, a three-dimensional potential energy function for $\tilde{X}^2A_1$ and $\tilde{A}^2B_1$ states of SiH_2^+ was constructed in 1994 by Bauer *et al.*[14] They also calculated the transition wavenumbers between $\tilde{X}^2A_1$ and $\tilde{A}^2B_1$ states based on the potential energy

*Project supported by the National Natural Science Foundation of China (Grant Nos. 11674198 and 11804193), the Shandong Provincial Natural Science Foundation of China (Grant No. ZR2019PA012), and the First-class Discipline Construction Foundation of Shandong Agricultural University.

†Corresponding author. E-mail: gaofeng@sdau.edu.cn
‡Corresponding author. E-mail: qtmeng@sdnu.edu.cn

© 2021 Chinese Physical Society and IOP Publishing Ltd

function, and the theoretical and experimental molecular parameters agree well. In 2002, Vach *et al.*[15] performed a molecular dynamics simulation to obtain the reactive cross sections of $Si^+(^2P)+H_2$ reaction in the collision range of 0.3 eV to 10 eV based on a semi-empirical PES of SiH_2^+ system. In 2004, Chaâbane *et al.*[16] carried out an investigation of molecular dynamics simulation with semi-empirical quantum chemistry on $Si^+(^2P)+H_2$ reaction in the energy range of 0.5 eV and 10 eV, and the reaction cross sections for different rotational and vibrational excitation of $H_2(v_0, j_0)$ and reaction mechanisms were discussed, which indicated the final energy distributions of the SiH^+ products were controlled by the initial translational, rotational and vibrational energies of H_2.

In this paper, based on the GMS-PES of $SiH_2^+(X^2A_1)$ system,[9] we carry out an accurate quantum dynamical calculation of $H+SiH^+$ reaction by using the Chebyshev wave packet method with considering full CC effect. Chebyshev wave packet can be used to study the systems with large mass due to the more advanced scaling laws over time-independent methods.[17–21] As the wave packet propagates in real space without approximation and reaction properties of all energy points can be calculated by a single wave packet propagation, the Chebyshev wave packet propagation scheme used in the present paper have been proved to be accurate and efficient.[18] The paper is organized as follows: the theoretical and computational methods used in this paper are described in Section 2. Section 3 presents the main results of the accurate quantum dynamics with considering full CC effect including reaction probabilities, integral cross sections (ICS) and rate constants for the title reaction and discusses in detail the influence of CC effect on the $SiH^+ + H$ reaction. Finally, Section 4 concludes the present work.

2. Theoretical approach

In the reactant $(H+SiH^+)$ Jacobi coordinates R (distance of H from the center of mass of SiH^+), r (internuclear distance of SiH^+) and γ (the angle between R and r), the Hamiltonian of $SiH_2^+(X^2A_1)$ system can be described as

$$H = -\frac{1}{2\mu_R}\frac{\partial^2}{\partial R^2} - \frac{1}{2\mu_r}\frac{\partial^2}{\partial r^2} + \frac{\hat{l}^2}{2\mu_R R^2} + \frac{\hat{j}^2}{2\mu_r r^2} + V(R,r,\gamma), \tag{2}$$

where the quantity $\mu_r = m_{Si}m_H/(m_{Si}+m_H)$ is the reduced mass of the SiH^+, $\mu_R = m_H(m_{Si}+m_H)/(2m_H+m_{Si})$ is the three-body reduced mass of the $H+SiH^+$ system, and $V(R,r,\gamma)$ is the interacting potential energy of $SiH_2^+(X^2A_1)$ system which can be obtained from PES. The rotational angular momentum operator and the orbital angular momentum operator of SiH^+ are denoted as $\hat{j}$ and $\hat{L}$, respectively, which can be expressed as

$$\hat{l}^2 = (\hat{J}-\hat{j})^2 = \hat{J}^2 + \hat{j}^2 - 2\hat{J}_z\hat{j}_z - \hat{J}_+\hat{j}_- - \hat{J}_-\hat{j}_+. \tag{3}$$

In Eq. (3), $\hat{J}$ denotes the total angular momentum operator, $\hat{J}_z$ and $\hat{j}_z$ are the body-fixed z components of total angular momentum operator and diatomic angular momentum operator, and $\hat{J}_+$ ($\hat{J}_-$) and $\hat{j}_+$ ($\hat{j}_-$) are the corresponding raising (lowering) operators. The last two terms in Eq. (3) are CC effect terms, which are ignored in CS approximation.

As neither discretization nor interpolation errors are introduced, the stable and accurate recursion relationship in the Chebyshev wave packet scheme are employed[18–21]

$$\begin{aligned} |\psi_{k+1}\rangle &= D\left(2\hat{H}_{norm}|\psi_k\rangle - D|\psi_{k-1}\rangle\right) \quad (k\geq 1), \\ |\psi_1\rangle &= D\hat{H}_{norm}|\psi_0\rangle, \end{aligned} \tag{4}$$

where $\hat{H}_{norm} = (\hat{H}-H^+)/H^-$ is the normalized Hamiltonian with $H^\pm = (H_{max}\pm H_{min})/2$, in which H_{max} (H_{min}) is the upper (lower) bounds of spectral range. The wave packets are multiplied with Gaussian shaped damping function at the grid edges to enforce the outgoing boundary condition,

$$D(x) = \begin{cases} 1, & x\leq x_d, \\ e^{-d_x(x-x_d)^2}, & x>x_d, \end{cases} \quad (x=R,r), \tag{5}$$

where x_d is the onset of the damping and d_x controls the extent of the damping. The initial wave packet is

$$|\psi_0\rangle = Ne^{-(R-R_0)^2/2\delta^2}\cos(k_0R)|\varphi_i\rangle. \tag{6}$$

In Eq. (6), N is normalization constant, k_0, R_0 and δ are initial momentum, central position and width of initial wave packet, respectively, and $|\varphi_i\rangle$ is a specific rovibrational eigenfunction.

By using a flux-based approach,[22] the initial state-specified total reaction probability is expressed as

$$P(E) = \frac{1}{2\pi\mu_r|a_i(E)|^2(H^-)^2\sin^2\theta} \times \mathrm{Im}\left\langle \sum_k (2-\delta_{k0})e^{-ik\theta}\psi_k \middle| \sum_{k'}(2-\delta_{k'0})e^{-ik'\theta}\left[\delta(r-r_f)\frac{\delta}{\delta r}\psi_{k'}\right]\right\rangle, \tag{7}$$

where $\theta \equiv \arccos\left((E-H^+)/H^-\right)$ is the Chebyshev angle, r_f defines the dividing surface in the product channel and $a_i(E)$ is the amplitude in the initial wave packet, which can be expressed as

$$a_i(E) = \left\langle i\sqrt{(\mu_R k_i/2\pi)}Rh_{li}^{(2)}(k_iR) \middle| \psi_0\right\rangle. \tag{8}$$

In Eq. (8), $h_{li}^{(2)}(k_iR)$ is the second order Hankel function.

The initial state-specified ICS is calculated by summing up the reaction probabilities for all quantum numbers J's of the total angular momentum for a given collision energy E_c

$$\sigma_{v_i j_i}(E_c) = \frac{\pi}{(2j_i+1)k^2_{v_i j_i}} \sum_{Jpl_i} (2J+1) P^{Jp}_{v_i j_i l_i}(E_c), \quad (9)$$

with $k^2_{v_i j_i} = 2\mu_R E_c$. $P^{Jp}_{v_i j_i l_i}(E_c)$ is the initial state-specified total reaction probability for the partial wave J and parity p at a given collision energy E_c. The initial states-specified rate constant is given by

$$k_{v_i j_i}(T) = \frac{f}{k_B T}\left(\frac{8}{\pi\mu_R k_B T}\right)^{1/2} \times \int_0^\infty \sigma_{v_i j_i}(E_c) e^{-E_c/k_B T} E_c \, dE_c, \quad (10)$$

where f, k_B, and T are the degeneracy factor, Boltzmann constant and the temperature, respectively.

3. Result and discussion

3.1. Potential energy surface and minimum energy path

The contour plots of $SiH_2^+(X^2A_1)$ system for bending angle $\angle[H–Si–H]^+ = 90°$ and collinear ($\angle[H–Si–H]^+ = 180°$) geometries are shown in Fig. 1. Obviously, a smooth behavior is exhibited at both long-range and short-range areas, which indicates the high quality of the GMS-PES. Due to the exchange symmetry of hydrogen atoms for the $SiH_2^+(X^2A_1)$ system, a perfectly symmetrical behavior is evident in Figs. 1(a) and 1(b). The remarkable feature is the local minimum located at about $R^+_{SiH} = R^+_{SiH'} = 2.80\ a_0$ in Fig. 1(a), which implies that there is a potential well for bending angle $\angle[H–Si–H]^+ = 90°$ geometry. In Fig. 1(b), there is a transition state at the $R^+_{SiH} = R^+_{SiH'} = 2.77\ a_0$ with an imaginary vibrational frequency of 1118.88i cm^{-1} for SiH^+ (SiH'^+) stretching mode and the saddle point at $R^+_{SiH} = 4.53\ a_0$ and $R^+_{SiH'} = 2.85\ a_0$ (or $R^+_{SiH} = 2.85\ a_0$ and $R^+_{SiH'} = 4.53\ a_0$).[9] As there is no deep potential well in Fig. 1(b), the linear $[H–Si–H]^+$ structure is not very stable.

The minimum energy paths (MEP) at fixed bending angle $\angle[H–Si–H]^+ = 90°$ and collinear ($\angle[H–Si–H]^+ = 180°$) geometries for $H + SiH^+ \rightarrow Si^+ + H_2$ reaction are depicted in Fig. 2. The MEP is defined as a function of the minimum potential energy varied with $R_{HH}R^+_{SiH}$ for $SiH_2^+(X^2A_1)$ system, where R_{HH} and R^+_{SiH} are the distances of H–H and Si–H^+ atoms, respectively. As can be seen, the energy released from the reactant $H + SiH^+$ to the product $Si^+ + H_2$ is about 1.32 eV, which implies that the title reaction is exoergic without threshold. The red solid line in Fig. 2 is the MEP for a perpendicular configuration ($\angle[H–Si–H]^+ = 90°$). There is only a deep well about 1.70 eV and no barrier exits in the perpendicular configuration, which is in accordance with the contour plot of Fig. 1(a). For a collinear approach (black dash), there is a deep well of about 1.40 eV and a barrier of about 0.20 eV. These features of the contour plot and MEP mentioned have decisive effects on dynamical behaviors of the title reaction, which will be discussed in detail below.

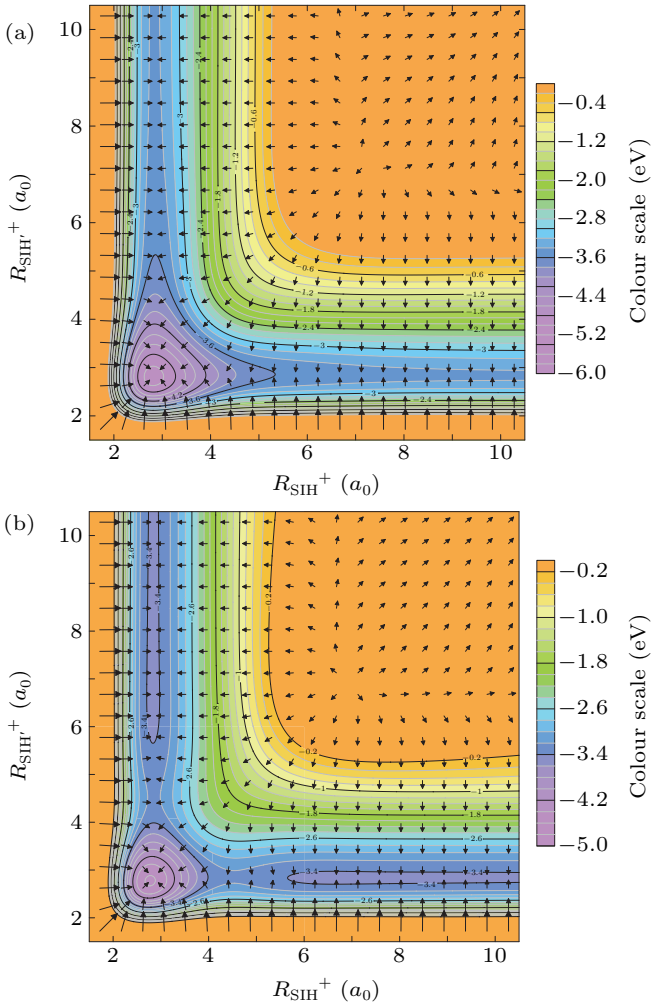


Fig. 1. Two contour plots for different configurations. (a) Contour lines for bending angle $\angle[H–Si–H]^+ = 90°$ figuration starting from −5.82 eV. (b) Contour lines for bending angle $\angle[H–Si–H]^+ = 180°$ starting from −4.63 eV. Both tow panels are drawn with an increment of 0.20 eV.

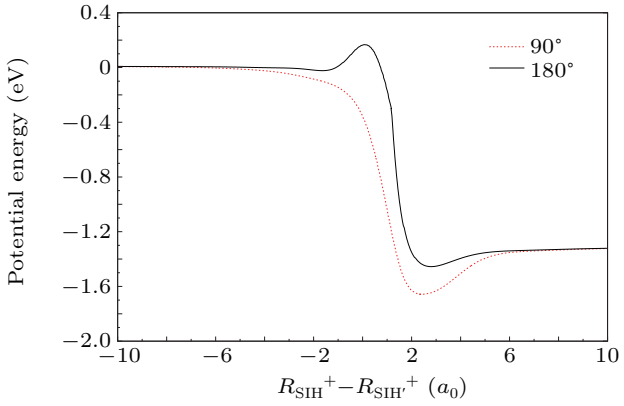


Fig. 2. The MEP of the different approaching angles ($\angle[H–Si–H]^+ = 90°$ & 180°) for $H + SiH^+ \rightarrow Si^+ + H_2$ reaction.

3.2. Reaction probabilities

By using the Chebyshev wave packet method, the accurate quantum dynamical investigation is employed on $H(^2S) +$

$SiH^+(X^1\Sigma^+) \rightarrow Si^+(^2P) + H_2(X^1\Sigma_g^+)$ reaction based on the GMS-PES for $SiH_2^+(X^2A_1)$ system. Through a systematic test of the convergence with $J = 0$, the optimum computational parameters in Jacobi coordinates are determined, which can be found in Ref. [9]. Due to the existence of deep potential well in reaction path and huge mass of $SiH_2^+(X^2A_1)$ system, the large computational parameters and plenty of partial waves bring out a huge challenge to our quantum dynamical calculations,[9] especially for the exact quantum calculations considering full CC effect. In order to get the exact ICSs and rate constants of the title reaction, the probabilities of all the partial waves up to $J = 90$ are calculated in the collision energy of 0 eV–1.0 eV. The number of partial waves in CS approximation is 100,[9] which is larger than the corresponding ones of exact calculations in the same collision energy range. As seen in Eqs. (2) and (3), the increment of centrifugal potential barrier becomes faster with the increase of J when the CC effect term is introduced into the Hamiltonian, which will reduce partial waves for exact quantum calculation in the same collision energy. In this work, the expensive computations are only carried out on probabilities of $J = 0, 5, 10, \ldots, 90$ for the title reaction, and the others are obtained by cubic spline interpolation method.[23]

The reaction probabilities of $J = 0$, 20, 40, 60 and 80 with exact quantum calculations are displayed in Fig. 3 for collision energy up to 1.0 eV. The distinctive feature is zero threshold for the probability of $J = 0$, which is owing to the barrierless insertion pathway of exothermic reaction. The reaction threshold shifts towards higher energy as J increases, which is consistent with J-shifting method[24] or capture model.[25,26] As so far, there are no experimental and other theoretical results of $H + SiH^+$ reaction compared with the results of this work, however, $H + CH^+$ reaction has been investigated extensively.[2,3,5,27,28] Furthermore, the topographical properties of $CH_2^+(1^2A')$ are essentially same with $SiH_2^+(X^2A_1)$ system,[4,9] hence, the variation tendency and resonance structure of reaction probability, ICS and rate constant of $H + SiH^+$ reaction are compared with the ones of $H + CH^+$ reaction.

As the same with the $H + CH^+$ reaction, the strong oscillation structures of reaction probabilities are displayed in Fig. 3, which can be attributed to the formation of a SiH_2^+ complex supported by stationary points of the $SiH_2^+(X^2A_1)$ PES.[9] The reaction probability oscillates strongly in the low energy range and the amplitude of oscillation is reduced with increment of collision energy presumably as the lifetimes of resonance states become shorter. Compared with $H + CH^+$ reaction, the oscillation amplitude of reaction probabilities for $H + SiH^+$ reaction is relatively smaller,[5] which is because that the potential well depth of SiH_2^+ system is shallower than that of CH_2^+ and the resonance amplitude is mainly determined by the potential well depth.[5,9] For example, the maximum depth of CH_2^+ system in C_{2V} symmetry is 4.74 eV,[9] which is larger than the potential well depth of SiH_2^+ system mentioned above. Although these two reactions are exoergic, the energy released for $H + SiH^+$ reaction is 1.32 eV, which is bigger than the exoergicity (0.496 eV) from the reactant $H + CH^+$ to the product $C^+ + H_2$. Therefore, the reaction probabilities of $H + SiH^+$ reaction are larger than the ones of $H + CH^+$ reaction overall.

As displayed in Fig. 4, the reaction probabilities for $J =$ 10, 20, 30, 40, 50, and 60 of the exact quantum calculations with considering full CC effect are compared with the corresponding results of CS approximation. Obviously, both CC and CS results show sharp oscillating structures in the collision energy of 0 eV–1.0 eV for $H + SiH^+$ reaction due to the deep well of SiH_2^+ system. However, the oscillation amplitudes of reaction probabilities for CC calculations are much smaller than the corresponding CS results. This is because that the CC effect dominated by long-range forces will increase the collision time by orientating the reactants and decrease the lifetime of resonance states.[11,29] For low J's ($J = 10$ and 20), the CC probabilities are larger than the CS ones at low collision energy (about $E_c \leq 0.75$ eV) and become slightly smaller than the CS results with the increment of collision energy. For high J's ($J =$ 30, 40, 50 and 60), the CC probabilities are smaller than the CS ones at low collision energy. When $J =$ 30, 40 and 50, the CC results are slightly larger than the CS ones at high collision energy (about $E_c \geq 0.70$ eV). While $J = 60$, the CC results are much larger than the CS ones above 0.55 eV. Overall, the differences between the CS and CC results are observed to be remarkable in the region where the reaction probabilities of CS fluctuate greatly. While, in the region with small oscillation of CS probabilities, the results of CC are basically consistent with those of CS. In CS approximation, SiH^+ molecule is confined to $k = 0$ (the projection of total angular momentum J onto the body-fixed z axis) quantum state, which will decrease the collision time, increase the resonances and lead to overestimation or underestimation of the reaction probability.[11,29,30]

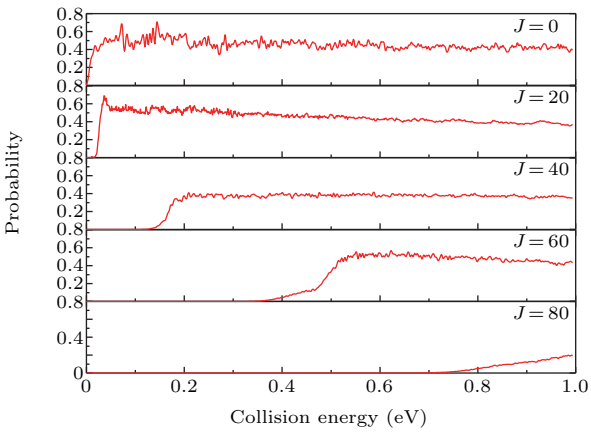


Fig. 3. The exact reaction probabilities varied with collision energy of 0 eV–1.0 eV for $J = 0$, 20, 40, 60 and 80.

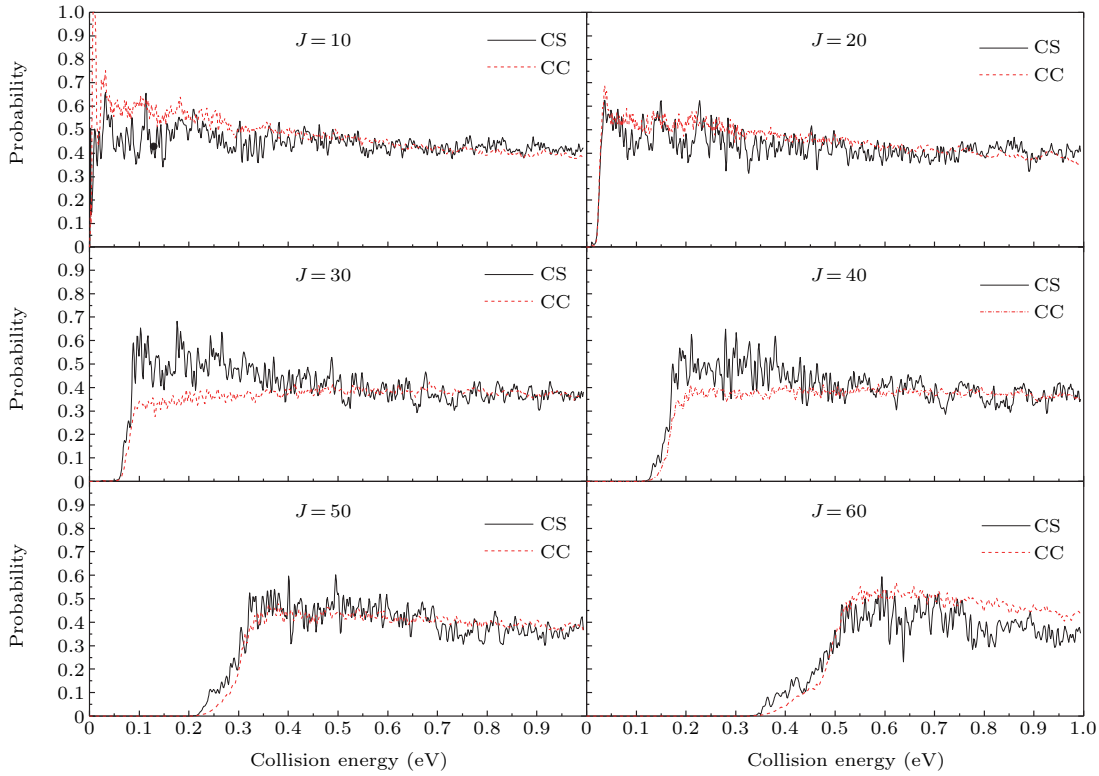


Fig. 4. The reaction probabilities of CC and CS calculations for $H + SiH^+ \rightarrow Si^+ + H_2$ reaction at $J = 10$, 20, 30, 40, 50, and 60.

3.3. Integral cross section and rate constant

The ICSs of CC and CS calculations are plotted over the collision energy range of 0 eV–1.0 eV in Fig. 5. It is obvious that both ICSs have no threshold. They decrease sharply with the increase of collision energy in the low energy region and then decrease slowly as collision energy increases. The trend of ICS for $H + SiH^+$ reaction varied with collision energy is similar to $H + CH^+$ reaction, which is determined by reaction mechanism of an exothermic reaction without potential barrier. After a weighted sum of all reaction probabilities, the oscillatory structure of ICS for CS approximation is still relatively obvious. While for CC ICS, the oscillatory structure has been smeared out mostly. As discussed in Ref. [29], CC effect has a significant influence on resonance by breaking the resonance complex. In the exact quantum calculation with considering full CC effect, ICS becomes smoother and less oscillating compared with the CS ones. In the collision energy range of 0 eV–0.05 eV, the ICSs of CC are much larger than CS ones. When 0.05 eV $\leq E_c <$ 0.1 eV, CS and CC ICSs are roughly equal. When 0.1 eV $\leq E_c <$ 0.5 eV, the CC results are slightly smaller than CS ones. When 0.5 eV $\leq E_c <$ 0.7 eV, the CC results are basically same with CS ones. When 0.7 eV $\leq E_c \leq$ 1.0 eV, the CC results are slightly larger than CS ones.

According to Eq. (10), the initial state specific ($v_i = 0$, $j_i = 0$) thermal rate constants for $H(^2S) + SiH^+(X^1\Sigma^+) \rightarrow Si^+(^2P) + H_2(X^1\Sigma_g^+)$ reaction are calculated from the energy resolved ICSs. The rate constants varied with temperature range from 5 K to 1000 K for both CC and CS calculations are displayed in Fig. 6. The rate constant of CC calculations increases sharply in the temperature range from 5 K to 75 K and then creeps up in the range of 75 K–175 K. From 175 K up to 1000 K, the CC result decreases slightly and are nearly constant. While for CS rate constant, a monotonic increasing behavior is shown. Overall, the CS result increases rapidly in the temperature range from 5 K to 100 K and then grows gradually above about 100 K. By comparison, CC and CS results are well consistent below 16 K. In the range of 16 K–100 K, CC rate constant increases more rapidly than CS ones, and the deviation of them becomes larger with the temperature increasing and reaches the maximum value about at 100 K. For instance, when $T = 25$ K, the CC rate constant is $k = 9.2 \times 10^{-10}$ cm^3·molecule$^{-1} \cdot$ s^{-1} the CS result is $k = 7.0 \times 10^{10}$ cm^3·molecule$^{-1} \cdot$ s^{-1}, and the relative error is 24.1%. When $T = 100$ K, the CC and CS rate constants are 1.7×10^{-9} and 9.4×10^{10} cm^3·molecule$^{-1} \cdot$ s^{-1}, respectively, and the relative error is 44.4%. In the range of 100 K–1000 K, the CC rate constant decreases slightly while the CS ones gradually increase, and the relative error of them obviously decreases. Compared with the reaction of $H + CH^+$, the rate constants of these two reactions are in the same order of magnitude at the same temperature, and further observation shows that the varied trend of CC rate constants of $H + SiH^+$ reaction is more similar to the ones of $H + CH^+$ collision.[3,5]

From the ICSs and rate constants discussed above, it can be seen that the deviation of CC and CS ICSs is small in the most of collision energy range except for the range 0 eV–

0.05 eV. But for rate constants, the deviation of them is considerable in the temperature range of 16 K–1000 K. In order to quantitatively investigate the effect of ICSs in the range of 0 eV–0.05 eV on the rate constants in the range of 0 K–1000 K, according to Eq. (10) the function of proportion $Pr(T)$ varied with temperature T is calculated by

$$Pr(T) = \frac{\int_{0.000001}^{0.05} E_c e^{-E_c/k_B T}\, dE_c}{\int_{0.000001}^{1} E_c e^{-E_c/k_B T}\, dE_c}, \tag{11}$$

where the numerator is the integration of partition function $E_c e^{-E_c/k_B T}$ over collision energy E_c below 0.05 eV, while the denominator is the total integration of 0.00001 eV–1 eV. In order to ensure the convergence of integral calculation, the lower limit of integration is 0.000001 instead of zero. The calculated function of proportion $Pr(T)$ varied with temperature T is displayed in Fig. 7.

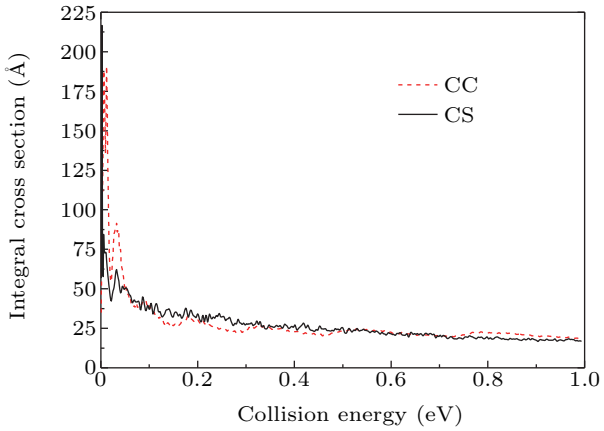


Fig. 5. The ICSs of CS and CC calculations for $H + SiH^+ \rightarrow Si^+ + H_2$ reaction over collision energy of 0 eV–1.0 eV.

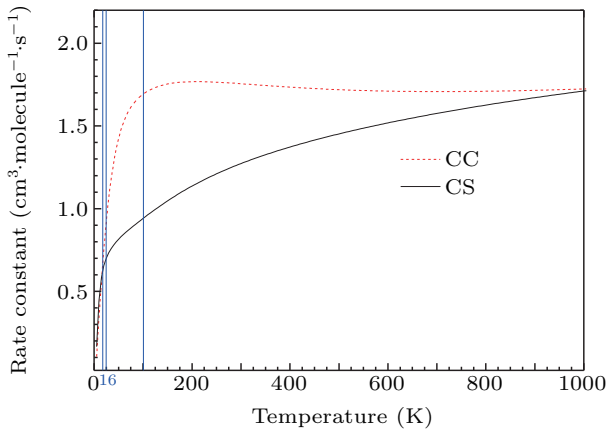


Fig. 6. The initial state ($v = 0$, $j = 0$) specified rate constant of $H + SiH^+ \rightarrow Si^+ + H_2$ reaction for CC and CS calculations obtained on the GMS PES.

In the above figures, the effect of ICSs in the range of 0 eV–0.05 eV on the rate constants in the range of 0 K–1000 K can be described as follows: when $0 < T \leq 16$ K, the effect is almost zero, so the CC and CS rate constants are basically same, and when $16 \leq T \leq 1000$ K, the contribution of ICSs in the range of 0 eV–0.05 eV to the rate constant at a given temperature drop from 100% to 11%. Especially in the temperature range of 16 K–250 K, the value of proportion function $Pr(T)$ is larger than 50% as displayed in Fig. 7, which indicates that the ICSs in the range of 0 eV–0.05 eV have a decisive effect on the rate constant. Therefore, it seems that the ICS of CC is consistent with the CS ones almost in the whole range of collision energy except for 0 eV–0.05 eV, but for rate constants, the deviation of CC and CS results is considerable in the temperature range of 16 K–1000 K. Considering the great gap between the rate constant of CS approximation and exact quantum calculation, it is believable that the CC effect is of great importance and cannot be ignored for $H(^2S) + SiH^+(X^1\Sigma^+) \rightarrow Si^+(^2P) + H_2(X^1\Sigma_g^+)$ reaction.

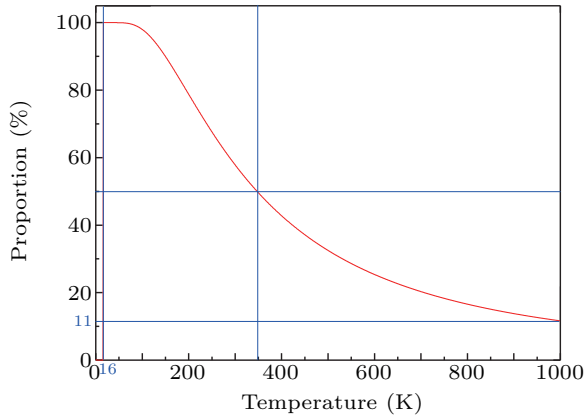


Fig. 7. The function of proportion $Pr(T)$ varied with temperature T.

4. Conclusion

Based on the global accurate GMS-PES of $SiH_2^+(X^2A_1)$, the Chebyshev quantum wave packet method is employed to study the dynamics of $H(^2S) + SiH^+(X^1\Sigma^+) \rightarrow Si^+(^2P) + H_2(X^1\Sigma_g^+)$ reaction in this work, and the initial state specified ($v = 0$, $j = 0$) probabilities, ICSs and rate constants are provided. The dynamical behaviors of these calculated results are according with an exothermic reaction without potential barrier. In order to investigate the effect of CC on the title reaction, a large number of partial waves ($J \leq 90$) in the collision energy range of 0 eV–1.0 eV are included, which brings out a huge challenge to exact quantum calculations with considering full CC effect. By comparing the CC probabilities with the corresponding CS ones, it is found that the CC effect dominated by long-range forces will increase the collision time by orientating the reactants and decrease the lifetime of resonance states, which means that neglecting CC effect will decrease the collision time, increase the amplitude of oscillation and lead to overestimation or underestimation of the reaction probability. For ICSs and rate constants, it is found that the deviation of CC and CS ICSs is small in the most of collision energy range except for the range of 0 eV–0.05 eV, while the deviation of both rate constants is considerable in the temperature range of

16 K–1000 K, which can be quantitatively illustrated by the function of proportion $Pr(T)$. In conclusion, the CC effect is of great importance and can not be ignored for the title reaction.

References

[1] Bender C F and Schaefer H F 1971 *J. Mol. Spectrosc.* **37** 423
[2] Stoecklin T and Halvick P 2005 *Phys. Chem. Chem. Phys.* **7** 2446
[3] Warmbier R and Schneider R 2011 *Phys. Chem. Chem. Phys.* **13** 10285
[4] Li Y Q, Zhang P Y and Han K L 2015 *J. Chem. Phys.* **142** 124302
[5] Sundaram P, Manivannan V and Padmanaban R 2017 *Phys. Chem. Chem. Phys.* **19** 20172
[6] Guo J, Zhang A J, Zhou Y, Liu J Y, Jia J F and Wu H S 2017 *Chem. Phys. Lett.* **689** 121
[7] Kasap S and Capper P 2017 *Springer Handbook of Electronic and Photonic Materials* (Heidelberg: Springer) pp. 573–576
[8] Zhang Y G, Dou G, Cui J and Yu Y 2018 *J. Mol. Struct.* **1165** 318
[9] Gao F, Zhang L L, Zhao W L, Meng Q T and Song Y Z 2019 *J. Chem. Phys.* **150** 224304
[10] Meijer A J H M and Goldfield E M 1999 *J. Chem. Phys.* **110** 870
[11] Chu T S and Han K L 2008 *Phys. Chem. Chem. Phys.* **10** 2431
[12] Elkind J L and Armentrout P B 1984 *J. Phys. Chem.* **88** 5454
[13] Curtis M C, Jackson P A, Sarre P J and Whitham C J 1985 *Mol. Phys.* **56** 485
[14] Bauer C, Hirst D M, Hall D I, Sarre P J and Rosmus P J 1994 *Chem. Sot. Faraday Trans.* **90** 517
[15] Vach H, Chaâbane N and Peslherbe G H 2002 *Chem. Phys. Lett.* **352** 127
[16] Chaâbane N, Vach H and Cabarrocas P R I 2004 *J. Phys. Chem. A* **108** 1818
[17] Zhang J Z H 1999 *Theory and Application of Quantum Molecular Dynamics* (World Scientific, Singapore) pp. 149–150
[18] Lin S Y and Guo H 2003 *J. Chem. Phys.* **119** 11602
[19] Gao F, Wang X L, Zhao W L, Song Y Z and Meng Q T 2018 *Eur. Phys. J. D* **72** 224
[20] Wang X L, Gao F, Gao S B, Zhang L L, Song Y Z and Meng Q T 2018 *Chin. Phys. B* **27** 043104
[21] Zhao W L, Wang Y G, Zhang L L, Yue D G and Meng Q T 2020 *Acta Phys. Sin.* **69** 083401 (in Chinese)
[22] Neuhauser D, Baer M, Judson R S and Kouri D J 1990 *J. Chem. Phys.* **93** 312
[23] Zhai H C and Lin S Y 2015 *Chem. Phys.* **455** 57
[24] Bowman J M 1991 *J. Phys. Chem.* **95** 4960
[25] Gray S K, Goldfield, E M, Schatz G C and Balint-Kurti G G 1999 *Phys. Chem. Chem. Phys.* **1** 1141
[26] Clary D C 1984 *Mol. Phys.* **53** 3
[27] Halvick Ph, Stoecklin T, Larregaray P and Bonnet L 2007 *Phys. Chem. Chem. Phys.* **9** 582
[28] Bovino S, Grassi T and Gianturco F A 2015 *J. Phys. Chem. A* **119** 11973
[29] De Fazio D and Castillo J F 1999 *Phys. Chem. Chem. Phys.* **1** 1165
[30] Lu R F, Wang Y H and Deng K M 2013 *J. Comput. Chem.* **34** 1735